Analytical Methods

A novel determination of curcumin via Ru@Au nanoparticles decorated nitrogen and sulfur-functionalized reduced graphene oxide nanomaterial

Journal:	*Analytical Methods*
Manuscript ID	AY-ART-11-2015-002950.R1
Article Type:	Paper
Date Submitted by the Author:	20-Nov-2015

Complete List of Authors:	Kotan, Gül; Kafkas University, Department of Chemistry Kardaş, Faruk; Erzincan University, Department of Science Education Yokuş, Özlem ; Kafkas University, Department of Science Education Akyıldırım, Onur; Kars University, Department of Chemical Engineering eren, tanju; Pamukkale University, Department of Chemical Engineering Yola, Mehmet; Sinop University, Atar, Necip; Pamukkale University, Deaprtment of Chemical Engineering; Saral, Hasan; Sinop University

A novel determination of curcumin via Ru@Au nanoparticles decorated nitrogen and sulfur-functionalized reduced graphene oxide nanomaterial

Gül Kotan[a], Faruk Kardaş[b], Özlem Aktaş Yokuş[c], Onur Akyıldırım[d], Hasan Saral[e], Tanju Eren[f], Mehmet Lütfi Yola[e,*], Necip Atar[f]

[a]*Department of Chemistry, Faculty of Science and Letters, Kafkas University, Kars, Turkey*

[b]*Department of Science Education, Faculty of Education, Erzincan University, Erzincan, Turkey*

[c]*Department of Science Education, Faculty of Education, Kafkas University, Kars, Turkey*

[d]*Department of Chemical Engineering, Faculty of Engineering and Architecture, Kafkas University, Kars, Turkey*

[e]*Department of Metallurgical and Materials Engineering, Faculty of Engineering, Sinop University, Sinop, Turkey*

[f]*Department of Chemical Engineering, Faculty of Engineering, Pamukkale University, Denizli, Turkey*

* To whom correspondence should be addressed:

Dr. Mehmet Lütfi Yola

Tel.: +90 3682715761; fax: +90 3682715763

E-Mail address: mehmetyola@gmail.com (M.L. Yola)

ABSTRACT

We report the synthesis of Ru@Au nanoparticles involved L-cysteine functionalized reduced graphene oxide (rGO) composite (NSrGO/Ru@AuNPs). The nanocomposites were characterized by transmission electron microscopy (TEM), scanning electron microscopy (SEM), X-ray photoelectron spectroscopy (XPS) and X-ray diffraction (XRD). The electrochemical determination of curcumin (CR) has been studied using square wave voltammetry (SWV) on glassy carbon electrode (GCE) modified with NSrGO/Ru@AuNPs composite (NSrGO/Ru@AuNPs/GCE). The effective surface areas (ESA) of rGO/GCE and NSrGO/Ru@AuNPs/GCE were calculated to be 347 cm^2/mg and 1289 cm^2/mg, respectively. These results show that the electrochemical surface area of the NSrGO/Ru@AuNPs/GCE is 3.71 times higher than those of rGO/GCE, respectively. The developed method was also applied successfully for the determination of CR in plasma and the linearity range of CR was 0.001 – 0.1 nM with the detection limit of 2.0×10^{-13} M.

Keywords: Curcumin; Human plasma, Reduced graphene oxide; Nanoparticles; Sensor

1. Introduction

CR [1,7-bis-(4-hydroxyl-3-methoxyphenyl)-1,6-heptadiene- 3,5-dione] is a phenolic pigment obtained from the rhizome of Curcuma longa Linn. CR has been found to exert the best inhibitory effects for various cancers by preventing the activation and proliferation of carcinogen and inducting apoptosis of the tumor cells [1]. CR is a potent substance with beneficial in vitro and in vivo effects, including antioxidant, antitumor, anti-inflammatory, antimicrobial, antiparasitic, antimutagenic, chemopreventive and chemotherapeutic activities [2-4]. Therefore, it is crucial to develope sensitive methods for determination of CR. Recently, number of analytical methods have been developed to detect CR with using high performance liquid chromatography [1], spectrophotometric [5] and liquid chromatography–mass spectrometry [6]. In addition, square wave voltammetry based on PdNps/Poly(Pr) nanocomposite was developed [7].

The important materials and nanoparticles in applications of nanotechnology can been used for the development of sensor, determination and catalytic effect [8-16]. In addition, significant progress has been performed in the production of carbon-supported materials with suitable cost. Nevertheless, there are some important problems such as low catalytic performance for analysis. Hence, in order to increase this performance, the novel nanomaterials such as graphene/graphene oxide become very significant [17-24].

In addition, some nanoparticles such as mono/bimetallic attracted important attention in nano/sensor technology. Because the nano-sized particles have larger specific surface area, they are good catalysts. The nanoparticles can also increase the rate of electrochemical reaction [25-27].

The voltammetric sensor based on NSrGO/Ru@AuNPs/GCE (Scheme 1) was firstly developed in this study. The preparation and characterization of nanocomposites were performed. After that, GCE surfaces were modified with these nanomaterials by using

infrared heat lamp. The developed electrochemical sensor was applied to plasma sample for the sensitive determination of CR.

2. Experimental

2.1. Materials

All chemicals that used in the experiments were reagent grade and were used as received following; Graphite powder (Merck, Germany), sulfuric acid (H_2SO_4, Merck, Germany), potassium persulfate ($K_2S_2O_8$, Merck, Germany), phosphorus pentoxide (P_2O_5, Merck, Germany), potassium permanganate ($KMnO_4$, Merck, Germany), hydrogen peroxide (H_2O_2, Merck, Germany), ethanol (Merck, Germany), hydrochloric acid (HCl, Sigma–Aldrich), N-(3-dimethylaminopropyl)-N′-ethylcarbodiimidehydrochloride (EDC, Sigma-Aldrich, USA), ethanol (Sigma-Aldrich, USA), $RuCl_3$ (Merck, Germany), ethylene glycol (Sigma-Aldrich, USA), L-cysteine (cis, Sigma–Aldrich, USA), $HAuCl_4$ (Sigma-Aldrich, USA), Sodium citrate (Merck, Germany), isopropyl alcohol (IPA, Sigma-Aldrich, USA), methanol (Merck, Germany), HPLC grade acetonitrile (MeCN, Sigma-Aldrich, USA), $NaBH_4$ (Merck, Germany), perchloric acid ($HClO_4$, Sigma-Aldrich, USA), $NH_2OH{\cdot}HCl$ (Merck, Germany) and other chemicals were reagent grade quality and were used as received. The ultra-pure water with resistance of 18.3 MΩ cm (Human Power 1^+ Scholar purification system) was used in the experiments of aqueous media.

2.2. Instrumentation

Square wave voltammetry (SWV) and cyclic voltammetry (CV) were carried out IviumStat (U.S) equipped with C3 cell stand. Electrochemical impedance spectroscopic experiments were carried out with Gamry Reference 600 workstation equipped with a PCI4/300 potentiostat in conjunction with EIS 300 software. Modified electrodes were characterized in 1.0 mM ferrocyanide/1.0 mM ferricyanide redox couple via EIS methods.

EIS data were measured at 100 kHz to 0.1 Hz at 10 mV wave amplitude and at an electrode potential of 0.155 V, the formal potential of ferrocyanide/ferricyanide redox couple.

JEOL 2100 HRTEM (JEOL Ltd., Tokyo, Japan) and ZEISS EVO 50 SEM (GERMANY) analytic microscopies were used to investigate the morphologies of GCE and NSrGO/Ru@AuNPs/GCE.

XPS analysis were performed on a PHI 5000 Versa Probe (Φ ULVAC-PHI, Inc., Japan/USA) model with monochromatized Al Kα radiation (1486.6 eV) as an X-ray anode operated at 50 W. To prepare the samples, one drop of the prepared NSrGO/Ru@AuNPs solutions were placed on clear glass and then dried in air.

A Rigaku Miniflex X-ray diffractometer was used for X-ray diffraction measurements of NSrGO/Ru@AuNPs nanostructures. A scanning speed of $2\theta = 2^0$/min with a step size of 0.02^0 was used to examine the samples.

2.3. Synthesis of rGO

GO was prepared by the modified Hummers method [9]. Typically, 2.5 g of graphite powder were placed in a flask containing a mixture of 12.5 mL of H_2SO_4 (98%), 2.5 g of $K_2S_2O_8$ and 2.5 g of P_2O_5. The mixture was kept at 80 °C for 6 h. Then, the mixture was cooled to room temperature and added with 500 mL of ultra-pure water. The product was filtered and washed with ultra-pure water and 125 mL of H_2SO_4 (98%) was added at 0 °C. Later, 15 g of $KMnO_4$ were added to the stirring suspension which was kept at 20 °C. After the feeding of $KMnO_4$ was finished, the flask was heated to 50 °C. After 4 h, 500 mL of ultra-pure water were added to the mixture in an ice bath. The last mixture was stirred for 2 h and diluted to 1 L with ultra-pure water. After that, the suspension was fed slowly with 20 mL of H_2O_2 (30%) and the solution started bubbling. The color of the suspension changed to brilliant yellow from brownish. The synthesized graphite oxide was filtered and washed with 0.1 M HCl and ultra-pure water three times. The graphite oxide was collected by an ultracentrifuge.

The as-prepared GO was dispersed into 200 mL water under mild ultrasound yielding a yellow-brown suspension, then 4 mL hydrazine hydrate (80 wt%) were added and the solution was heated in an oil bath maintaining at 100 °C under a water-cooled condenser for 24 h. After the reaction, the prepared rGO product was collected by vacuum filtration.

2.4. Synthesis of Ru@AuNPs

The Ru^{3+} ions in the $RuCl_3$ solution were reduced by adding PVP into ethylene glycol solution. The RuNPs was prepared by heating at 100 ^{o}C in a microwave reactor (Model CEM discover SP-D, CEM Corporation, Matthews, NC) until the color of the solution turns into dark brown . After that, 0.45 mM 50 mL $HAuCl_4$ and 6.25 mM 50 mL $NH_2OH{\cdot}HCl$ solutions were added drop by drop to the as-prepared RuNPs solution under room temperature. Ru@AuNPs was prepared by stirring the mixture until the color was turned into lilac from dark brown.

2.5. Preparation of NSrGO/Ru@AuNPs nanohybrid

rGO was dissolved in ethanol at 2 mg mL^{-1}. The mixture was sonicated to form a homogeneous suspension. The prepared rGO suspension was treated with 0.2 M of EDC solution for 8 h to ensure the surface activation of residual carboxylated groups. EDC compound provides the most popular and versatile method for labeling or crosslinking to free carboxylic groups on rGO. The EDC molecules are considered zero-length carboxyl-to-amine crosslinkers. EDC reacts with carboxylic acid groups to form an active intermediate product that is easily displaced by nucleophilic attack from primary amino groups in the reaction mixture. The primary amine forms an amide bond with the original carboxyl group, and an EDC by-product is released as a soluble derivative. Therefore, we used EDC for activation of free carboxylic acid groups of rGO. Then 1.0 mM cysteine was mixed with the activated rGO suspension at a 1:1 volume ratio and kept stirring for 2 h (NSrGO).

After that, 1 mg mL^{-1} of Ru@AuNPs solution was mixed with the 0.1 mg mL^{-1} of NSrGO solution at a 1:1 volume ratio. Finally, the mixture was sonicated to generate a homogeneous mixture (NSrGO/Ru@AuNPs). The mixture was then kept undisturbed under ambient condition for 24 h (Scheme 1).

Here Scheme 1

2.6. Procedure for the electrode preparation

Glassy carbon electrodes were cleaned by polishing with fine wet emery paper. They were polished with 0.1 μm and 0.05 μm alumina slurries, respectively on microcloth pads. The electrodes were sonicated twice in ultra-pure water and then in 50:50 (v/v) IPA and MeCN solution. After washing with water, glassy carbon electrode was washed with MeCN to eliminate any physisorbed materials. NSrGO/Ru@AuNPs nanohybrid modified GCE was prepared using an infrared heat lamp. 20 μL of NSrGO/Ru@AuNPs nanohybrid suspensions was dropped onto the GCE and then evaporating the solvent under an infrared heat lamp. The electrochemical characterizations of GCE, rGO/GCE and NSrGO/Ru@AuNPs/GCE were performed by cyclic voltammetry (CV) between -0.1 and +0.9 V. The square wave voltammograms of CR were performed by using the NSrGO/Ru@AuNPs/GCE as working electrode in the present study. The NSrGO/Ru@AuNPs/GCE was stored in closed box without fluctuations of temperature and pressure. The Ag/AgCl(aq) and Pt wire electrodes were utilized as reference and counter electrode, respectively.

2.7. Sample preparation

The empty plasma samples in this study were obtained from Hacettepe University Hospitals Blood Bank Unit in TURKEY. After the various standard CR solutions were added to these empty plasma samples, plasma samples were spiked:1.2 mL methanol was added to an aliquot of 0.4 mL plasma sample in a 2.0 mL plastic centrifuge tube. After that, the centrifugation at 20000 rpm for 15 min was performed. The upper clear layer solution was

diluted with 0.1 M acetate buffer (pH 5.0) for analysis. The informed consent will be obtained for improved experimentation with human subjects in future.

3. Results and discussion

3.1. Characterizations of nanohybrid

The morphologies of the Ru@AuNPs and NSrGO/Ru@AuNPs nanohybrid were investigated by using the JEOL 2100 HRTEM with an accelerating voltage of 200 keV. A drop of sample solution was deposited on a polymeric grid at room temperature under an argon gas stream. Fig. 1A shows the TEM image of Ru@AuNPs. In the Ru@AuNPs morphology, the darker nucleus assigns to the RuNPs and the lighter shell assigns to the AuNPs. Fig 1B shows the transparent, creased and planar sheet like morphology of rGO. Fig 1B confirms that the Ru@AuNPs have been seen as dark dots with a mean diameter of 10 to 30 nm on rGO sheets.

Here Figure 1

The morphology of the NSrGO/Ru@AuNPs/GCE surface was characterized by SEM. Fig 2A shows the smooth surface of bare GCE. Fig 2B shows dense layers on the electrode surface, indicating that the successful binding of NSrGO/Ru@AuNPs nanohybrid.

Here Figure 2

Fig. 3 shows the XPS spectrum of NSrGO/Ru@AuNPs nanohybrid, C_{1s}, N_{1s}, S_{2p}, Ru_{3p} and Au_{4f} peaks are prominent, showing that Ru@AuNPs have been functionalized on N- and S- involved rGO sheets. The C_{1s} core-level XPS spectrum of the nanohybrid was curve-fitted in Fig. 3. The peaks at 283.4 eV, 284.3 eV and 286.4 eV are assigned to -CH and -CN and -CONH, respectively. The peak located at 397.4 eV in the N_{1s} narrow region is corresponded to C–N groups in the covalent attachment of the carboxyl group of the rGO with the amino group of the L-cysteine [11]. S_{2p} region was curve-fitted with two components by a doublet ($2p^{1/2}$ and $2p^{3/2}$), owing to the spin-orbit coupling [11]. The peak at 162.1 eV indicated that the

sulfur atom in the nanohybrid was grafted to AuNPs. The peak at 163.2 eV can be assigned to free mercapto group in unreacted L-cysteine [11, 26]. Ru_{3p} narrow region was characterized by doublet $3p^{3/2}$ and $3p^{1/2}$ signals that appear at 462.3 and 485.4 eV, respectively. These peaks confirm the presence of RuNPs on NSrGO/Ru@AuNPs nanohybrid. The peak signals at 83.1 and 87.7 eV are corresponded to Au $4f^{7/2}$ and $4f^{5/2}$, respectively, indicating the functionalization of gold with sulfur group of the L-cysteine on rGO sheets [8].

Here Figure 3

The successful synthesis of NSrGO/Ru@AuNPs nanohybrid was also confirmed by XRD patterns in Fig 4. The intense and narrow peaks at $2\theta = 31.77^{o}$ and 44.82^{o} refers to the (002) and (004) planes of rGO sheets, respectively. The characteristic peaks of AuNPs also have been observed with the peaks at $2\theta=37.58^{o}$, 43.11^{o}, 62.07^{o} and 76.24^{o} that corresponded to the (111), (200), (220) and (311) planes of gold, respectively. The peaks at $2\theta=37.58^{o}$, 43.11^{o}, 62.07^{o} are corresponded to the Ru(101)-Au(111), Ru(200)-Au(200) and Ru(220)-Au(220) planes, respectively.

Here Figure 4

3.2. Cyclic voltammograms of CR at different electrode surfaces

Fig. 5 shows the cyclic voltammetry of 1.0×10^{-6} M CR in 0.1 M acetate buffer (pH 5.0) at different electrode surfaces. A couple of redox peaks was obtained at E_a of about 600 mV with peak-to-peak separation, ΔE_p, about 400 mV for CR at GCE. Nevertheless, the anodic and cathodic peaks at the GCE modified reduced graphene oxide without L-cysteine were much greater than those at GCE. The main oxidation peaks were more pronounced at reduced graphene oxide without L-cysteine than at GCE. In addition, when incorporating of Ru@AuNPs onto the surfaces of L-cysteine functionalized reduced graphene oxide, the well-behaved anodic and cathodic peaks were obtained for CR. As a result of the presence of Ru@AuNPs, an obvious increase in the background current was observed and the anodic peak

and cathodic peak increased. Hence, we can say that NSrGO/Ru@AuNPs/GCE can greatly accelerate the electron transfer rate between CR molecules in solution and the surface. CR gave oxidation peak at E_a of 520 mV with ΔE_p of 270 mV. The peak currents of the oxidation and reduction were about four larger than those obtained at GCE with the well separation. The following reasons might explain the electrocatalytic response of CR at the NSrGO/Ru@AuNPs/GCE. According to the literature, there are important problems for ultra-sensitive analysis. In order to increase the performance of analysis, novel nanomaterial such as rGO was used in this study. These enhanced performances were corresponded to the large surface area and good electrical conductivity of rGO and the synergistic effect of rGO and metal nanoparticles [25, 28]. In addition, the electrical properties of rGO showed that rGO was very sensitive to surface adsorbates, thus making rGO a promising platform for highly sensitive sensors [29]. Hence, rGO is conductive and has chemically active defect sites making it a promising candidate for the active material in molecular sensor.

Here Figure 5

The ESA of different modified electrodes was obtained by CV with 1.0 mM $[Fe(CN)_6]^{3-}$ solution containing 0.1 M KCl as a probe at different scan rates according to the equation: $i_p = 2.69\times10^5\ A\ n^{3/2}\ D^{1/2}\ C\ v^{1/2}$, where i_p refers to the peak current and A is the electrode area (cm^2). For 1.0 mM $[Fe(CN)_6]^{3-}$, n = 1, D = 7.6×10^{-6} cm^2 s^{-1} (0.1 M KCl), C is the concentration of $[Fe(CN)_6]^{3-}$, v is the scan rate. The ESA of rGO/GCE and NSrGO/Ru@AuNPs/GCE were calculated from the slope of the i_p versus $v^{1/2}$ plot to be 347 cm^2/mg and 1289 cm^2/mg, respectively. These results show that the electrochemical surface area of the NSrGO/Ru@AuNPs/GCE is 3.71 times higher than those of rGO/GCE, respectively. The high activity was explained by the small size of NSrGO/Ru@AuNPs.

3.3. Characterization of modified electrodes by EIS

EIS is an effective method for probing the features of surface modified electrodes. It is capable of giving useful information about defects/holes exist on the modified surfaces, the kinetics and mechanism of the film formation processes and surface coverage [30-32]. Fig. 6 shows the impedance plot (Nyquist diagram) of the bare GCE, rGO/GCE and the NSrGO/Ru@AuNPs/GCE. In addition, the inset of Fig. 6 shows the experimental data that are fitted to standard Randles equivalent circuits for NSrGO/Ru@AuNPs/GCE surface analysis, which comprises the solution resistance (R_s), the charge transfer resistance (R_{ct}) and the constant phase element (CPE) for the cases of NSrGO/Ru@AuNPs/GCE. The EIS graph (curve a of Fig. 6) demonstrated that the value of charge transfer resistance (R_{ct}) of bare GCE was calculated as 250 ohm. When the bare GCE was modified with rGO, the value of R_{ct} was lower (150 ohm) (curve b of Fig. 6). Because of the lower value, we can say that the rGO increases the rate of electron transfer. When NSrGO nanocomposite was modified with Ru@AuNPs, the value of R_{ct} of NSrGO/Ru@AuNPs/GCE was lower than that of rGO/GCE (curve c of Fig. 6). Thus, the addition of Ru@AuNPs shows the increase of catalytic activity. In addition, the charge transfer resistance at the rGO/GCE is higher than that at the NSrGO/Ru@AuNPs/GCE as estimated, indicating the active property of the NSrGO/Ru@AuNPs film.

Here Figure 6

3.4. Analytical application

The square wave voltammograms in 0.10 M acetate buffer (pH 5.0) containing 0.001, 0.005, 0.01, 0.02, 0.05 and 0.1 nM of CR on NSrGO/Ru@AuNPs/GCE are presented in Fig. 7A. The peak currents are linear with CR concentrations from 1.0×10^{-12} - 1.0×10^{-10} M. The regression equation of CR (Fig. 7B) is y = 315.4x + 0.721 (y is peak current, μA; x is CR

concentrations, nM; the number of data points is 6). Each point of the calibration graph corresponded to the mean value obtained from 6 independent measurements.

Limit of quantification (LOQ) was estimated by the equation:

$$LOQ = 10\ S / m,$$

Limit of detection (LOD) was estimated by the equation**:**

$$LOD = 3.3\ S / m,$$

Where *S* is the standard deviation of the intercept and *m* is the slope of the regression line [33, 34]. The limit of quantitation for CR was found to be 1.0×10^{-12} M and the calculated detection limit for CR was found to be 2.0×10^{-13} M. Data of the calibration curve was given in Table 1.

Here Figure 7

Table 1. Data of the calibration curve for the prepared electrochemical sensor (n = 6)

	CR
Regression equation	y = 315.4x + 0.721
Standard error of the slope	0.4
RSD of the slope	0.31
Standard error of the intercept	0.006
RSD of the intercept	2.04
Correlation coefficient (r)	0.9995
Linearity range (M)	1.0×10^{-12} - 1.0×10^{-10}
Number of data points	6
LOD (M)	2.0×10^{-13}
LOQ (M)	1.0×10^{-12}

y = ax + b; y: SWV signal (μA), x: CR concentration (nM), a: slope, b: intercept, LOQ: Limit of quantification, LOD: Limit of detection, RSD: % Relative Standard Deviation

The performance of prepared electrochemical sensor is comparable with the values reported by other research groups. Table 2 presents a comparison of the sensor performance in

terms of linear range and LOD with other analytical methods. It is seen that the developed sensor showed a much lower limit of detection.

Table 2. Comparison of different methods for CR detection

Method	Linear range for CR (mol/L)	LOD for CR (mol/L)	Reference
HPLC	2.1×10^{-7}-41.6×10^{-6}	4.16×10^{-8}	1
Spectrophotometric	2.7×10^{-9}-2.7×10^{-8}	2.7×10^{-9}	5
PdNps/Poly(Pr)/GE	5.0×10^{-9}-1.0×10^{-7}	1.2×10^{-9}	7
GR/GCE	5.0×10^{-8}-3.0×10^{-6}	3.0×10^{-8}	35
LC-MS/MS	6.8×10^{-9}- 5.4×10^{-6}	6.75×10^{-9}	6
NSrGO/Ru@AuNPs/GCE	*1.0×10^{-12} - 1.0×10^{-10}*	*2.0×10^{-13}*	*This study*

The NSrGO/Ru@AuNPs/GCE was applied to spiked plasma samples to investigate applicability of modified electrode. The concentration values of CR in plasma was calculated to be $6.61\pm(0.03)\times10^{-11}$ M for six repeated measurements by NSrGO/Ru@AuNPs/GCE. Liquid chromatography coupled with mass spectrometry was selected as reference method [6]. The concentration value of CR in plasma was calculated to be $6.53\pm(0.06)\times10^{-11}$ M by liquid chromatography coupled with mass spectrometry. The results obtained by NSrGO/Ru@AuNPs/GCE are in well agreement with those obtained by liquid chromatography coupled with mass spectrometry. The results demonstrate the applicability of the NSrGO/Ru@AuNPs/GCE for determination of CR in the presence of the other excipients. In addition, the standard addition technique was applied to the same preparations which were analysed by calibration curves. The regression equations of standard addition curve were found to be y = 318.37x + 10.512 for CR in spiked plasma. It is clear that there is no

significant difference between slopes of calibration curves and standard addition curves. These results showed that there was no interference from matrix components.

In addition, in order to evaluate the effects of other excipients on the proposed method, the experiments of recoveries were performed. The recoveries for sample solutions are presented in Table 3. Closeness of the results to 100.00% showed that recovery of the method was very good for real samples. Therefore, the developed method is highly selective for the determination of CR.

Table 3. The recoveries of CR in plasma samples (n=7)

Sample	Added CR (nM)	Found CR (nM)	Recovery (%)
Plasma	-	0.661±(0.03)	-
	0.01	0.673(± 0.01)	101.66 ± 1.4
	0.02	0.679(± 0.05)	102.41 ± 1.1
	0.03	0.662(± 0.03)	99.70 ± 0.7

In addition, the developed sensor was applied to blank solution, 0.1 nM standard CR and plasma sample containing 0.10 nM CR to investigate matrix effect. The voltammogram obtained from human plasma sample containing 0.1 nM CR was identical with the voltammogram obtained from standard solution containing an equivalent of CR (Fig. 8). Thus, we can say that highly selective sensor is specific to the target molecule.

Here Figure 8

3.5. Repeatability, Reproducibility and Stability of the NSrGO/Ru@AuNPs/GCE

In order to show the repeatability of NSrGO/Ru@AuNPs/GCE, ten adsorption-regeneration cycles were repeated in the presence of 0.1 nM CR. According to the results, NSrGO/Ru@AuNPs/GCE has demonstrated the repeated signals during the ten cycles. For reproducibility study, six different NSrGO/Ru@AuNPs modified electrodes were prepared

under the same condition and tested in CR detection. After that, each electrode was applied to human plasma samples for CR analysis. According to the obtained results, the RSD is 0.44% in 0.1 nM CR. The stability of NSrGO/Ru@AuNPs/GCE was also checked. After 30 days, the signal was found to be approximate 99.13% of the original value which suggests its excellent long-term stability.

4. Conclusion

We developed the voltammetric sensor for determination of curcumin on NSrGO/Ru@AuNPs modified GCE. The prepared nanomaterials and surfaces were well characterized by TEM, SEM, EIS, CV, XRD and XPS. According to the results, the voltammetric sensor was accomplished homogeneously on the glassy carbon surface. The developed sensor showed high sensitivity towards curcumin with the detection limit of 2.0×10^{-13} M. In addition, the prepared sensor is reusable, selective and stable. In particular, the prepared sensor offers the advantages of simplicity and efficiency in target detection. A high percentage of recovery shows that the developed sensor can be used to quantify curcumin without interference. In conclusion, the voltammetric sensor is sensitive, rapid, cheap and easy to use and might be preferred to the analytical methods.

References

1. Y. Long, W. Zhang, F. Wang and Z. Chen, *Journal of Pharmaceutical Analysis*, 2014, **4**, 325-330.
2. H. Hatcher, R. Planalp, J. Cho, F. M. Torti and S. V. Torti, *Cellular and Molecular Life Sciences*, 2008, **65**, 1631-1652.
3. S. Bengmark, *Journal of Parenteral and Enteral Nutrition*, 2006, **30**, 45-51.
4. Y. S. Huang, T. J. Hsieh and C. Y. Lu, *Food Chemistry*, 2014, **174**, 571-576.
5. N. K. Gupta, A. Nahata, V. K. Dixit, *Asian Journal of Traditional Medicines*, 2010, **5**, 12-18.

6. P. Ramalingam and Y. T. Ko, *Journal of Chromatography B*, 2014, **969**, 101-108.

7. E. Arslan and S. Çakır, *J Solid State Electrochem*, 2014, **18**, 1611-1620.

8. M. L. Yola and N. Atar, *Electrochimica Acta*, 2014, **119**, 24-31.

9. M. L. Yola, T. Eren and N. Atar, *Electrochimica Acta*, 2014, **125**, 38-47.

10. N. Atar, T. Eren and M. L. Yola, *Thin Solid Films*, 2015, **590**, 156-162.

11. N. Atar, T. Eren, B. Demirdögen, M. L. Yola and M. O. Çağlayan, *Ionics*, 2015, **21**, 2285-2293.

12. N. Atar, T. Eren, M. L. Yola, H. Karimi-Maleh and B. Demirdögen, *RSC Advances*, 2015, **5**, 26402-26409.

13. R. Jain, V. K. Gupta, N. Jadon and K. Radhapyari, *Analytical Biochemistry*, 2010, **407**, 79-88.

14. R. N. Goyal, V. K. Gupta and S. Chatterjee, *Sensors and Actuators B: Chemical*, 2010, **149**, 252-258.

15. V. K. Gupta, A. Nayak, S. Agarwal and B. Singhal, *Combinatorial Chemistry and High Throughput Screening*, 2011, **14**, 284-302.

16. V. K. Gupta, A. K. Jain, L. P. Singh and U. Khurana, *Analytica Chimica Acta*, 1997, **355**, 33-41.

17. V. K. Gupta, T. Eren, N. Atar, M. L. Yola, C. Parlak and H. Karimi-Maleh, *Journal of Molecular Liquids*, 2015, **208**, 122-129.

18. M. L. Yola, T. Eren and N. Atar, *Sensors and Actuators, B: Chemical*, 2015, **210**, 149-157.

19. V. K. Gupta, M. L. Yola, N. Atar, Z. Üstündağ and A. O. Solak, *Journal of Molecular Liquids*, 2014, **191**, 172-176.

20. V. K. Gupta, M. L. Yola, N. Atar, Z. Ustundağ and A. O. Solak, *Electrochimica Acta*, 2013, **112**, 541-548.

21. V. K. Gupta, N. Atar, M. L. Yola, M. Eryılmaz, H. Torul, U. Tamer, İ. H. Boyacı and Z. Üstündağ, *Journal of Colloid and Interface Science*, 2013, **406**, 231-237.

22. V. K. Gupta, A. K. Jain, S. Agarwal and G. Maheshwari, *Talanta*, 2007, **71**, 1964-1968.

23. H. Khani, M. K. Rofouei, P. Arab, V. K. Gupta and Z. Vafaei, *Journal of Hazardous Materials*, 2010, **183**, 402-409.

24. M. L. Yola, N. Atar, T. Eren, H. Karimi-Maleh and S. Wang, *RSC Advances*, 2015, **5**, 65953-65962.

25. M. L. Yola, T. Eren and N. Atar, *Biosensors and Bioelectronics*, 2014, **60**, 277-285.

26. M. L. Yola, V. K. Gupta, T. Eren, A. E. Şen and N. Atar, *Electrochimica Acta*, 2014, **120**, 204-211.

27. V. K. Gupta, M. L. Yola, T. Eren, F. Kartal, M. O. Çağlayan and N. Atar, *Journal of Molecular Liquids*, 2014, **190**, 133-138.

28. V. K. Gupta, N. Atar, M. L. Yola, Z. Üstündağ and L. Uzun, *Water Research*, 2014, **48**, 210-217.

29. A. Lipatov, A. Varezhnikov, P. Wilson, V. Sysoev, A. Kolmakov and A. Sinitskii, *Nanoscale*, 2013, **5**, 5426-5434.

30. V. K. Gupta, M. L. Yola, N. Özaltın, N. Atar, Z. Üstündağ and L. Uzun, *Electrochimica Acta*, 2013, **112**, 37-43.

31. V. K. Gupta, M. L. Yola, N. Atar, A. O. Solak, L. Uzun and Z. Üstündağ, *Electrochimica Acta*, 2013, **105**, 149-156.

32. V. K. Gupta, M. L. Yola, M. S. Qureshi, A. O. Solak, N. Atar and Z. Üstündağ, *Sensors and Actuators B: Chemical*, 2013, **188**, 1201-1211.

33. M. L. Yola and N. Özaltin, *Reviews in Analytical Chemistry*, 2011, **30**, 29-36.

34. M. L. Yola and N. Özaltin, *Revista de Chimie*, 2011, **62**, 420-426.

35. K. Li, Y. Li, L. Yang, L. Wang and B. Ye, *Analytical Methods*, 2014, **6**, 7801-7808.

Figure captions

Scheme 1. The procedure for fabrication of NSrGO/Ru@AuNPs/GCE

Figure 1. TEM image of (A) Ru@AuNPs and (B) NSrGO/Ru@AuNPs nanohybrid

Figure 2. SEM image of (A) bare GCE, (B) NSrGO/Ru@AuNPs/GCE surfaces

Figure 3. The narrow region XPS spectra of C_{1s}, N_{1s}, S_{2p}, Ru_{3p} and Au_{4f} of NSrGO/Ru@AuNPs nanohybrid

Figure 4. XRD characterization of NSrGO/Ru@AuNPs nanohybrid

Figure 5. Cyclic voltammograms of CR at GCE, GCE modified rGO and NSrGO/Ru@AuNPs/GCE in sodium acetate/acetic acid buffer solution of pH 5.0. Concentration of each analyte: 1.0 μM (Scan rate is 100 mV s^{-1})

Figure 6. Fitting of impedance spectrum for 1.0 mM $[Fe(CN)_6]^{3-/4-}$ (1:1) in 0.1 M KCl at (a) GCE, (b) rGO/GCE and (c) NSrGO/Ru@AuNPs/GCE. Inset is the Randles equivalent circuit. Frequency range is 100000 – 0.1 Hz with 10 mV wave amplitude at a formal potential of 0.155 V. RE stands for reference electrode and WE stands for working electrode.

Figure 7. (A) Square wave voltammograms on NSrGO/Ru@AuNPs/GCE in sodium acetate/acetic acid buffer solution of pH 5.0, (B) The calibration curve of CR

Figure 8. Square wave voltammograms of electrochemical sensor towards (a) blank solution, (b) 0.10 nM standard CR solution and (c) human plasma sample containing 0.10 nM CR in sodium acetate/acetic acid buffer solution of pH 5.0

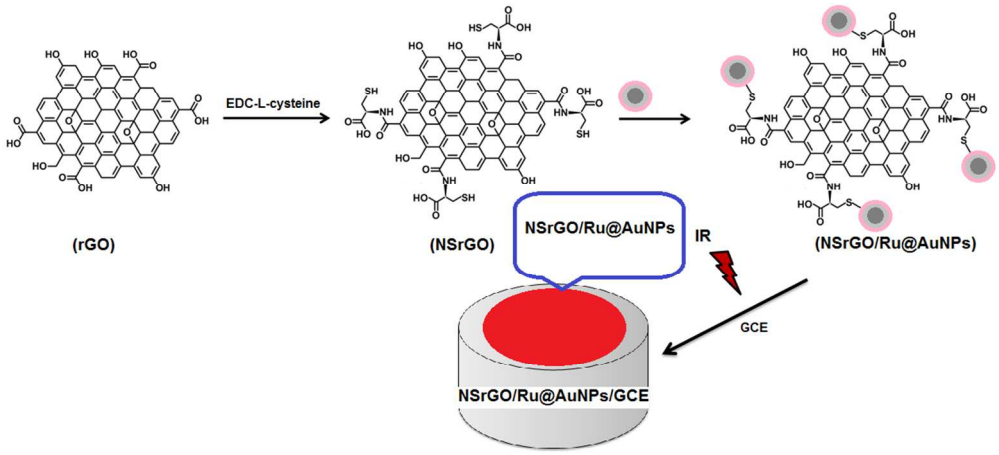

334x150mm (96 x 96 DPI)

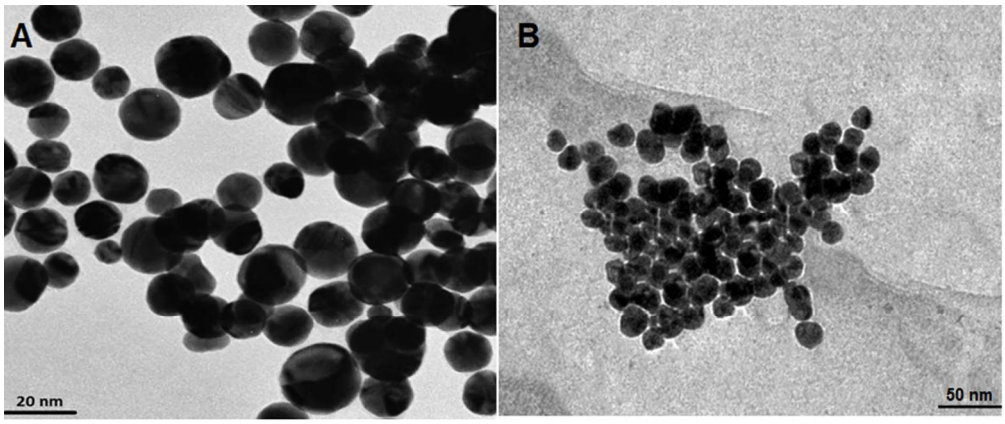

231x96mm (96 x 96 DPI)

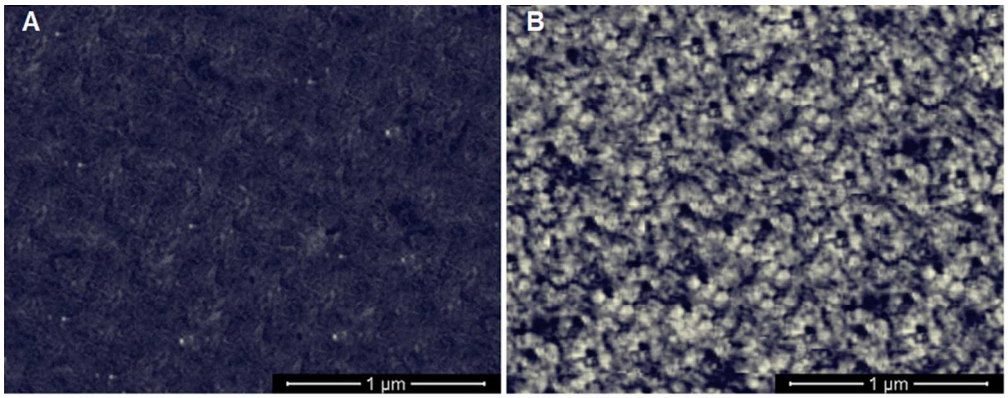

287x114mm (96 x 96 DPI)

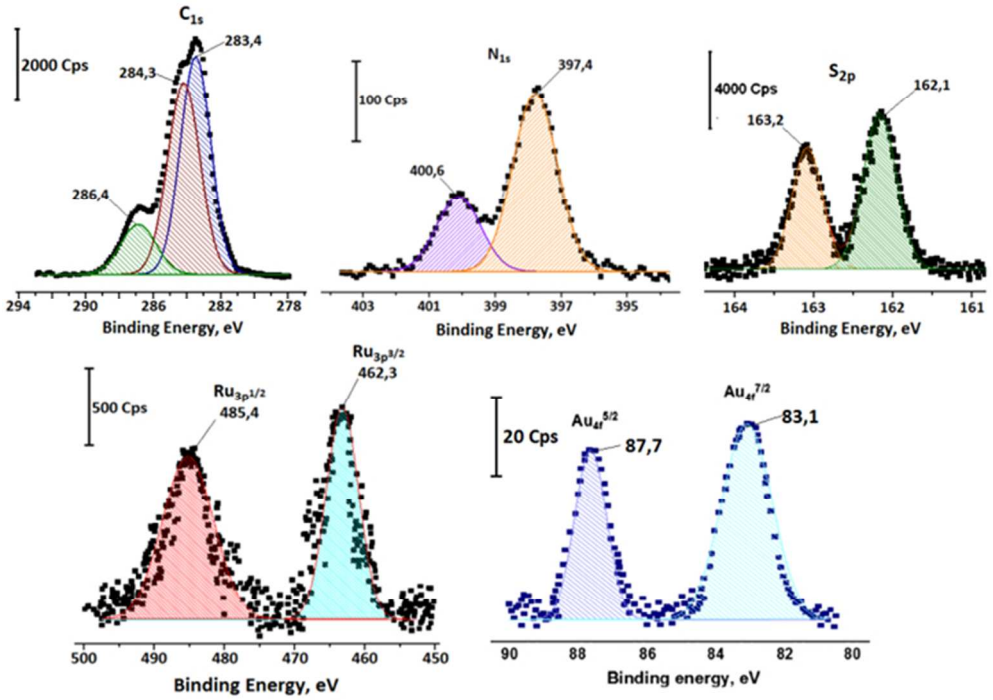

193x135mm (96 x 96 DPI)

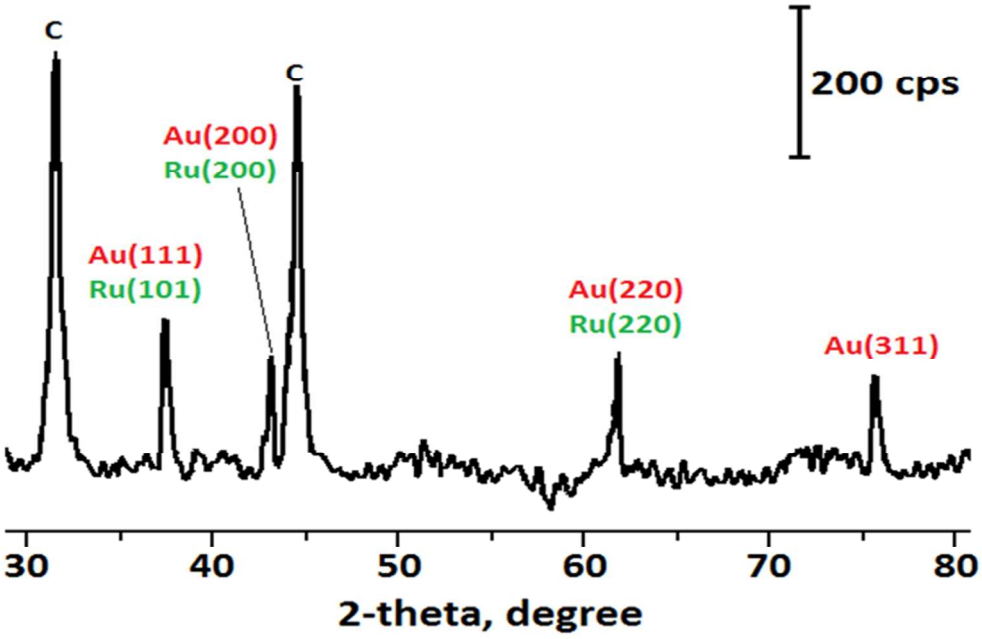

201x132mm (96 x 96 DPI)

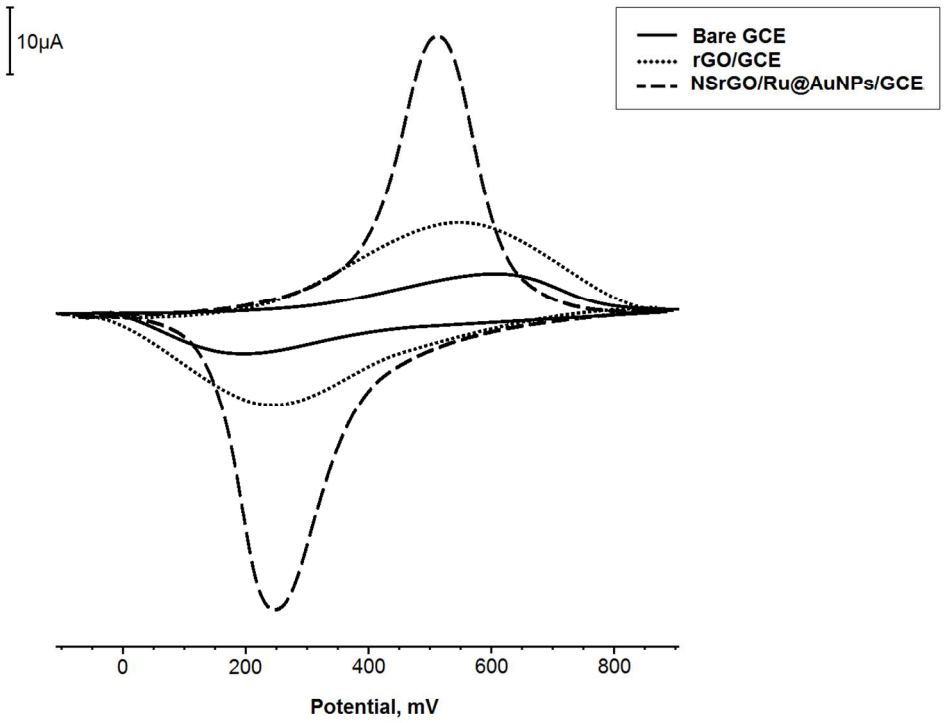

379x284mm (96 x 96 DPI)

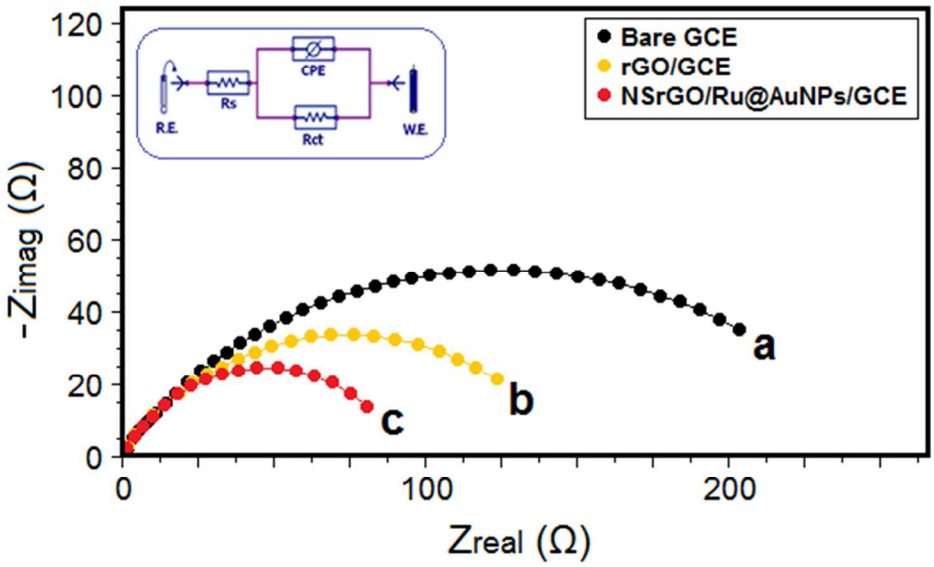

160x98mm (96 x 96 DPI)

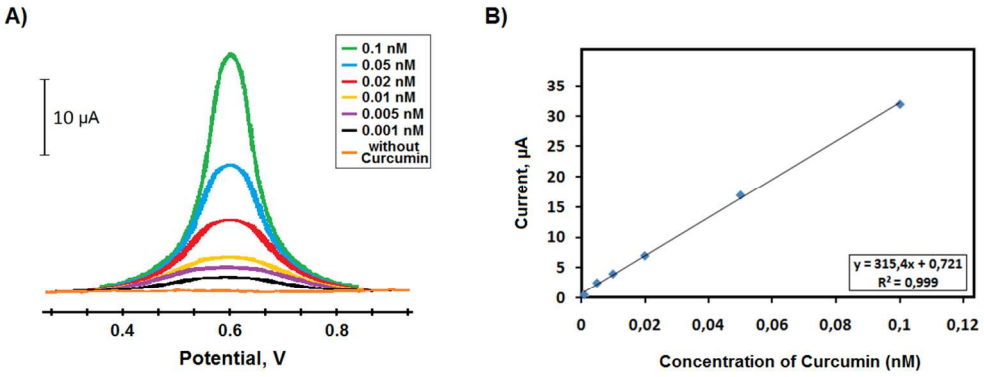

327x130mm (96 x 96 DPI)

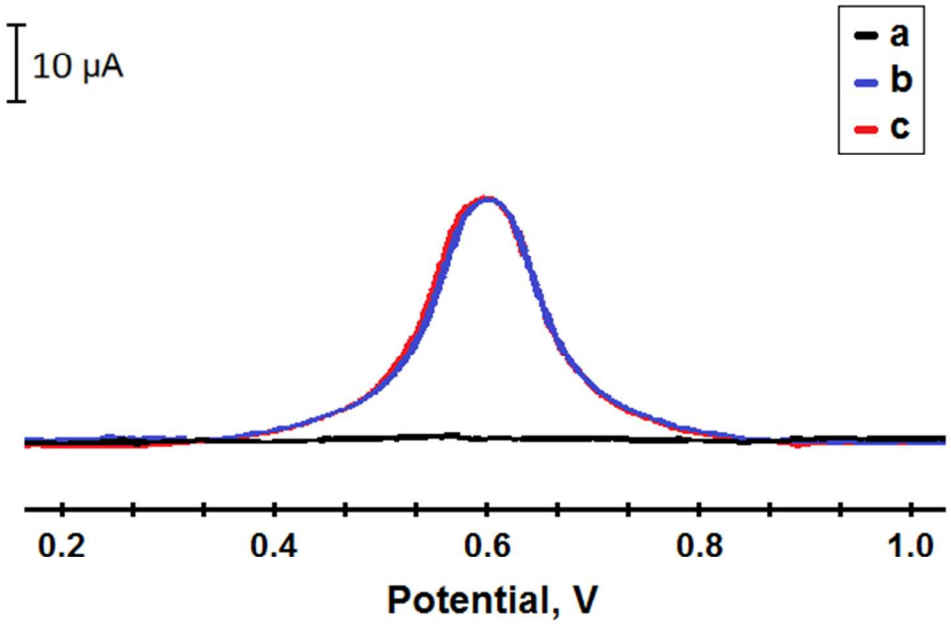

164x115mm (96 x 96 DPI)

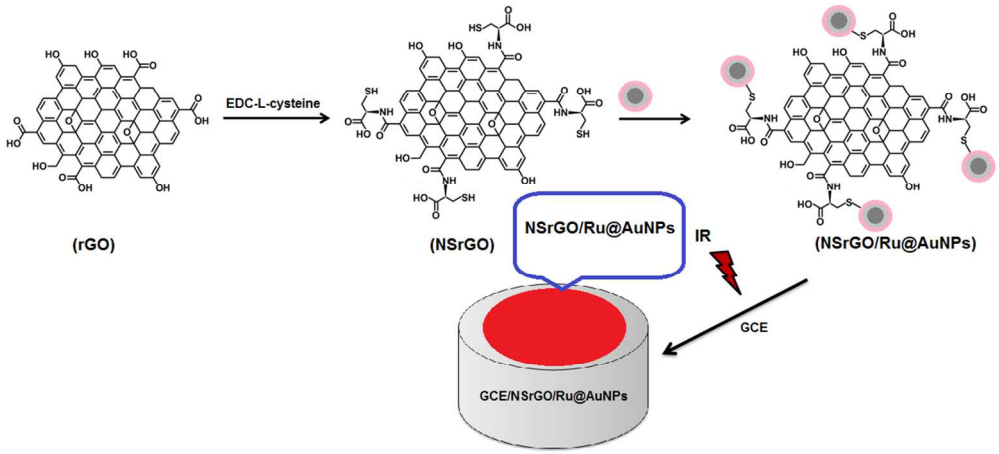
EDC-L-cysteine
(rGO)
(NSrGO)
(NSrGO/Ru@AuNPs)
NSrGO/Ru@AuNPs
IR
GCE
GCE/NSrGO/Ru@AuNPs